

A novel approach for modelling the cluster detector and the SPI spectrometer

RITESH KSHETRI* and PINTU BHATTACHARYA

Department of Physics, Sidho-Kanho-Birsha University, Ranchi Road, P.O. Sainik School, Purulia 723 104, India

*Corresponding author. E-mail: ritesh.kshetri@gmail.com

DOI: 10.1007/s12043-014-0883-6; ePublication: 30 October 2014

Abstract. A probabilistic approach has been presented in six recent papers (R Kshetri, *J. Instrum.* 2012 7 P04008; *ibid.*, P07006; *ibid.*, P07008; *ibid.*, P08015; *ibid.*, P12007; *Appl. Radiat. Isotopes* 2013 75 30) for modelling a general composite detector. In this paper, a simplistic view has been presented on the application of our formalism to composite detectors consisting of hexagonal closely packed encapsulated HPGe detector modules. We have presented modified calculations for the peak-to-total (PT) and peak-to-background (PB) ratios of the cluster and spectrometer for integral satellite (SPI) for the first time considering up to four-fold events. Instead of using an empirical method or simulation, we present a novel approach for calculating the peak-to-total ratio of the SPI spectrometer for high γ energies. Our work can provide guidance for designing new composite detectors and for performing experimental studies with the SPI spectrometer for high-energy γ -rays.

Keywords. SPI spectrometer; cluster detector; γ -rays; peak-to-total ratio; peak-to-background ratio; phenomenological modelling.

PACS Nos 87.53.Bn; 07.85.Fv; 88.50.gj; 95.55.–n

1. Introduction

The gamma spectrometer for INTEGRAL satellite, addresses the fine spectroscopy of celestial γ -ray sources. It consists of an array of 19 closely packed encapsulated high-purity germanium (HPGe) detectors surrounded by an active anticoincidence shield of bismuth germanate [1]. The cluster detector is a similar composite detector, which consists of seven closely packed encapsulated HPGe detectors inside the same cryostat [2].

For γ energies from 10 keV to 10 MeV, three types of interactions are important for γ -ray detection [2]: the photoelectric absorption, the Compton scattering and the pair production (possible when γ -ray energy ≥ 1.022 MeV). The full energy peak (FEP) corresponds to the complete absorption of incident γ energy and gets contributions from

photoelectric absorption in a single step and from the Compton scattering or/and the pair production where all scattered γ -rays are finally absorbed in the detector. When a γ -ray interacts with a composite detector, its energy can be deposited completely in a single detector module or there is partial deposition of γ energy in several detector modules. As a result, the composite detector can be operated in the single detector mode and the addback mode [2]. Note that the number of individual detector modules that participate in one FEP event is called the fold. The latter mode corresponds to events where the full γ -ray energy is deposited by single and multiple fold events. Due to these multiple fold events, the FEP efficiency and peak-to-total (PT) ratio are higher in addback mode compared to single detector mode (where energy is deposited by single-fold events only).

The HPGe detector modules of the cluster and SPI spectrometers have different single crystal volumes – for a cluster detector, a single crystal has a volume of 286 cm³, while a SPI single crystal has a volume of 178 cm³. The high-energy response of these two spectrometers for high-energy γ -rays have been determined by Wilhelm *et al* [3] and Attie *et al* [1], respectively. During these measurements, the source-to-detector distance for the cluster and SPI detectors were 0.25 and 125 m, respectively. In spite of having different single crystal volumes, as a result of different distance of operation, the variation of relative efficiency in single detector and addback modes is quite similar for these two detectors (see discussion on figure 2 in [4]). As a result, it is possible to use the experimental data of Wilhelm *et al* [3] for cluster detector and predict the response of SPI spectrometer. This is shown in our recent works [4–7] where a phenomenological approach of detector modelling has been used. Remarkable agreement between theoretical and experimental results has been observed for the SPI spectrometer at various energies [4–7]. The effect of shape and size of composite detectors on the peak-to-total and peak-to-background ratios, is shown in [6]. Similar approaches for modelling the simplest composite detector – the clover detector are presented in [8,9].

This work mainly deals with the calculation of the PT ratio by considering up to four-fold events and the experimental data of the cluster detector for γ energies up to 8 MeV. In this paper, we have reviewed our approach of [4,5]. Our approach and the predictions from our calculations can provide a guidance for experimental studies with the SPI spectrometer for high-energy γ -rays.

2. The formalism

We assume that inside a general composite detector having K modules ($K = 7$ and 19 for the cluster and SPI spectrometers, respectively), the hexagonal HPGe detector modules have identical shape, size and are placed symmetrically [4,5,7]. Let N_T be the total flux of monoenergetic γ -rays incident on the composite detector such that, at a time a single γ -ray can interact with a detector module. Let N be the portion of the total flux that interacts with the detector module of the composite detector. For the N γ -rays (of energy E_γ) incident on the detector module, let the probability of scattering away from the detector without detection be S'_o , the probability of scattering to adjacent detectors be S'_i and the probability of full energy peak absorption be A' , such that $S'_o + A' + S'_i = 1$.

Regarding second and higher interactions with modules, let us consider all possible FEP events, where an incident γ -ray of energy E_o is absorbed after multiple detector interactions. Considering an average over energy and scattering angle of possible scattered γ -rays after the first and higher interactions with detector modules, we observe that the scattered γ -rays after the first, second and higher interactions show the same detector volume for interaction. So, for simplicity, we can assume that the interaction probabilities for secondary and higher interactions of γ -rays with the modules remain constant. We assume that each detector module can either absorb (with FEP absorption probability A) or scatter a γ -ray away from its volume (with probability S_o for leaving the detector without detection and probability S_i for scattering to adjacent detectors), such that $A + S_o + S_i = 1$. We have separated the single interaction probabilities from multiple ones because on an average the γ -rays before and after the first interaction have different detector volumes.

2.1 Modelling of the cluster detector

In a cluster detector, we have two groups of detector modules – six outer detectors and one central detector, as shown in figure 1. Let N_o and N_c represent the γ flux that interacts with the six outer and one central detector module(s), respectively. So, we have $N_o = 6N$ and $N_c = N$. Let the probability amplitudes for an outer detector be $A', S'_{io}, S'_{oo}, A, S_{io}, S_{oo}$ and the ones for central detector be represented by $A', S'_{ic}, S'_{oc}, A, S_{ic}, S_{oc}$. Note that the absorption probability remains the same.

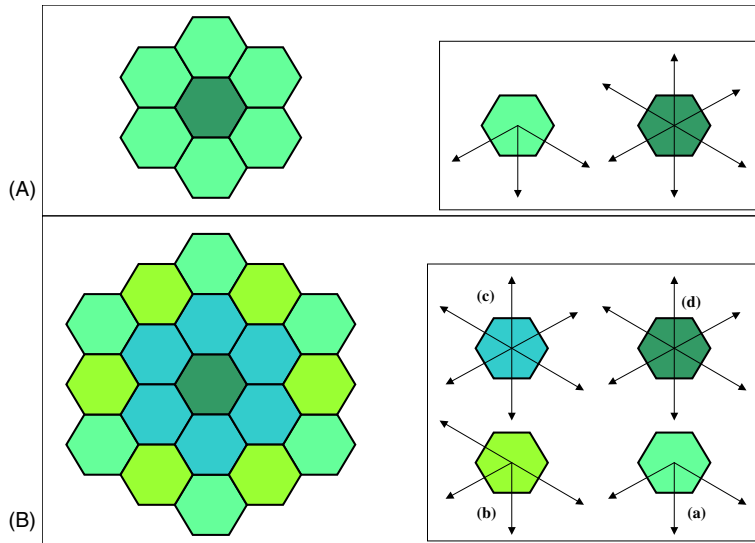


Figure 1. The cluster detector and the SPI spectrometer are schematically shown in figures (A) and (B), respectively. Inset shows possible γ -ray scatterings from different groups of detector modules to adjacent modules.

From the scattered events ($N_o S'_{io}$), $\frac{2}{3}$ rd events can enter the two adjacent outer detectors and $\frac{1}{3}$ rd events can enter the central detector so that,

$$\begin{aligned} S'_{io} &= S'_{io} \left[\frac{2}{3}(A + S_{io} + S_{oo}) + \frac{1}{3}(A + S_{ic} + S_{oc}) \right] \\ &= S'_{io} \left[A + \frac{1}{3}\{(2S_{io} + S_{ic}) + (2S_{oo} + S_{oc})\} \right]. \end{aligned} \quad (1)$$

After the second interaction, the absorbed events and events scattered to adjacent detectors are given by

$$N'_o = N_o \left[\{A' + S'_{io}A\} + \frac{1}{3}S'_{io}(2S_{io} + S_{ic}) \right]. \quad (2)$$

Similar to eq. (1),

$$S_{io} = S_{io} \left[A + \frac{1}{3}\{(2S_{io} + S_{ic}) + (2S_{oo} + S_{oc})\} \right]. \quad (3)$$

The scattered events from the central detector can enter the six outer detectors, so that

$$S_{ic} = S_{ic}(A + S_{io} + S_{oo}). \quad (4)$$

Using the above expressions, after the third interaction, the absorbed events and events scattered to adjacent detectors are given by

$$\begin{aligned} N''_o &= N_o[A' + S'_{io}A] + \frac{1}{3}N_o S'_{io} \left[2S_{io} \left\{ A + \frac{1}{3}(2S_{io} + S_{ic}) \right\} + S_{ic}(A + S_{io}) \right] \\ &= N_o \left[\left\{ A' + S'_{io}A + \frac{1}{3}S'_{io}(2S_{io} + S_{ic})A \right\} + \frac{1}{9}S'_{io}S_{io}(4S_{io} + 5S_{ic}) \right]. \end{aligned} \quad (5)$$

Thus, after the fourth interaction, the absorbed events are

$$N'''_o = N_o \left[A' + S'_{io}A + \frac{1}{3}S'_{io}(2S_{io} + S_{ic})A + \frac{1}{9}S'_{io}S_{io}(4S_{io} + 5S_{ic})A \right]. \quad (6)$$

Let us consider the case of the central detector. After the first interaction, we have

$$N_c = N_c S'_{oc} + N_c A' + N_c S'_{ic}. \quad (7)$$

All the scattered events can enter the six outer detectors, so that

$$S'_{ic} = S'_{ic}(A + S_{io} + S_{oo}). \quad (8)$$

After the second interaction, the absorbed events and events scattered to adjacent detectors are given by

$$N'_c = N_c [\{A' + S'_{ic}A\} + S'_{ic}S_{io}]. \quad (9)$$

Using eq. (5), after the third interaction, the absorbed events and events scattered to adjacent detectors are given by

$$N''_c = N_c \left[A' + S'_{ic}A + S'_{ic}S_{io} \left\{ A + \frac{1}{3}(2S_{io} + S_{ic}) \right\} \right]. \quad (10)$$

After the fourth interaction, the absorbed events are

$$\begin{aligned}
 N_c''' &= N_c \left[A' + S'_{ic} A + S'_{ic} S_{io} \left\{ A + \frac{1}{3} (2S_{io} + S_{ic}) A \right\} \right] \\
 &= N_c \left[A' + S'_{ic} A + S'_{ic} S_{io} A + \frac{1}{3} S'_{ic} S_{io} (2S_{io} + S_{ic}) A \right]. \tag{11}
 \end{aligned}$$

From the symmetry of the detector configuration, it can be observed that if the probability amplitudes for the central detector are $A', S'_i, S'_o, A, S_i, S_o$, then the corresponding amplitudes for each outer detector should be $A', \frac{1}{2}S'_i, (\frac{1}{2}S'_i + S'_o), A, \frac{1}{2}S_i, (\frac{1}{2}S_i + S_o)$. Using these amplitudes and substituting the values of N_o and N_c , the counts corresponding to the absorbed events (after the fourth interaction) are given by

$$N''' = N_o''' + N_c''' = 7N[A' + \alpha_{clu}], \tag{12}$$

where

$$\begin{aligned}
 \alpha_{clu} &= \frac{4}{7}AS'_i + \frac{5}{14}AS'_iS_i + \frac{3}{14}AS'_iS_i^2 \\
 &= AS'_i[0.57 + 0.36S_i + 0.21S_i^2]. \tag{13}
 \end{aligned}$$

2.2 Modelling of the SPI spectrometer

If we analyse different inward scatterings of γ -rays, then the SPI spectrometer can be considered to consist of four groups of detector modules as shown by different colours of figure 1. The details for each case are shown in table 1. We have also calculated and shown the expressions for scattering probability to the adjacent modules. In each of these expressions, the term which gives the probability to scatter away from the modules, is not shown because it will not effect α . Let N_a, N_b, N_c and N_d represent the γ flux that interacts with the detector module(s) of types (a), (b), (c) and (d), respectively. Considering figure 1 and table 1, we have $N_a = 6N, N_b = 6N, N_c = 6N$ and $N_d = N$.

Table 1. Distribution of scattered events to adjacent detector modules is shown for different types of detector modules of the SPI spectrometer. Corresponding expressions for scattering probability to the adjacent modules are also shown.

| Type of modules | Number of modules | Distribution of scattered events | Expression for scattering probability to the adjacent detector modules |
|-----------------|-------------------|---|---|
| a | 6 | $\frac{2}{3}b + \frac{1}{3}c$ | $S_{ia} = S_{ia} \left[A + \frac{1}{3}(2S_{ib} + S_{ic}) \right] + (\dots)$ |
| b | 6 | $\frac{1}{2}a + \frac{1}{2}c$ | $S_{ib} = S_{ib} \left[A + \frac{1}{2}(S_{ia} + S_{ic}) \right] + (\dots)$ |
| c | 6 | $\frac{1}{3}b + \frac{1}{3}c + \frac{1}{6}a + \frac{1}{6}d$ | $S_{ic} = S_{ic} \left[A + \frac{1}{6}(2S_{ib} + 2S_{ic} + S_{ia} + S_{id}) \right] + (\dots)$ |
| d | 1 | c | $S_{id} = S_{id}[A + S_{ic}] + (\dots)$ |

Let us consider the six detector modules of type (a). After the first interaction, we have

$$\begin{aligned} N_a &= N_a S'_{oa} + N_a A' + N_a S'_{ia} \\ &= N_a A' + N_a S'_{ia} + (\dots). \end{aligned} \tag{14}$$

Here we have not shown the term depending on probability to scatter away from the modules because it will never effect α . The expression for S'_{ia} is similar to S_{ia} shown in table 1. Using this expression, after the second interaction, we have

$$\begin{aligned} N_a &= N_a A' + N_a S'_{ia} \left[A + \frac{1}{3}(2S_{ib} + S_{ic}) \right] + (\dots) \\ &= N_a (A' + S'_{ia} A) + \frac{N_a}{3} S'_{ia} (2S_{ib} + S_{ic}) + (\dots). \end{aligned} \tag{15}$$

Using expressions for S_{ib} and S_{ic} from table 1, after the third interaction, we get

$$\begin{aligned} N_a &= N_a (A' + S'_{ia} A) + \frac{N_a}{3} S'_{ia} \left[2S_{ib} \left\{ A + \frac{1}{2}(S_{ia} + S_{ic}) \right\} \right. \\ &\quad \left. + S_{ic} \left\{ A + \frac{1}{6}(2S_{ib} + 2S_{ic} + S_{ia} + S_{id}) \right\} \right] + (\dots). \end{aligned} \tag{16}$$

Thus, the absorbed events after the fourth interaction are

$$\begin{aligned} N_a''' &= N_a (A' + S'_{ia} A) + \frac{N_a}{3} A S'_{ia} \left[2S_{ib} \left\{ 1 + \frac{1}{2}(S_{ia} + S_{ic}) \right\} \right. \\ &\quad \left. + S_{ic} \left\{ 1 + \frac{1}{6}(2S_{ib} + 2S_{ic} + S_{ia} + S_{id}) \right\} \right] \\ &= N_a \left[A' + \frac{1}{2} S'_i A + \frac{7}{18} A S'_i S_i + \frac{65}{216} A S'_i S_i^2 \right]. \end{aligned} \tag{17}$$

Similarly, after the fourth interaction, the absorbed events for other cases are

$$\begin{aligned} N_b''' &= N_b [A' + A S'_{ib}] + \frac{N_b}{2} A S'_{ib} \left[S_{ia} \left\{ 1 + \frac{1}{3}(2S_{ib} + S_{ic}) \right\} \right. \\ &\quad \left. + S_{ic} \left\{ 1 + \frac{1}{6}(2S_{ib} + 2S_{ic} + S_{ia} + S_{id}) \right\} \right] \\ &= N_b \left[A' + \frac{2}{3} A S'_i + \frac{1}{2} A S'_i S_i + \frac{43}{108} A S'_i S_i^2 \right], \end{aligned} \tag{18}$$

$$\begin{aligned} N_c''' &= N_c [A' + A S'_{ic}] + \frac{N_c}{6} A S'_{ic} \left[2S_{ib} \left\{ 1 + \frac{1}{2}(S_{ia} + S_{ic}) \right\} \right. \\ &\quad \left. + 2S_{ic} \left\{ 1 + \frac{1}{6}(2S_{ib} + 2S_{ic} + S_{ia} + S_{id}) \right\} \right. \\ &\quad \left. + S_{ia} \left\{ 1 + \frac{1}{3}(2S_{ib} + S_{ic}) \right\} + S_{id} \{ 1 + S_{ic} \} \right] \\ &= N_c \left[A' + A S'_i + \frac{29}{36} A S'_i S_i + \frac{2}{3} A S'_i S_i^2 \right], \end{aligned} \tag{19}$$

$$\begin{aligned}
 N_d''' &= N_d[A' + AS'_{id}] + N_dAS'_{id}S_{ic} \left\{ 1 + \frac{1}{6}(2S_{ib} + 2S_{ic} + S_{ia} + S_{id}) \right\} \\
 &= N_d \left[A' + AS'_i + AS'_iS_i + \frac{29}{36}AS'_iS_i^2 \right]. \tag{20}
 \end{aligned}$$

From the symmetry of the detector configuration, it can be observed that if the probability amplitudes for the central detector (type (d)) are $A', S'_i, S'_o, A, S_i, S_o$, then the corresponding amplitudes for detectors of type (c) should be $A', S'_i, S'_o, A, S_i, S_o$, amplitudes for detectors of type (b) should be $A', \frac{2}{3}S'_i, (\frac{1}{3}S'_i + S'_o), A, \frac{2}{3}S_i, (\frac{1}{3}S_i + S_o)$ and amplitudes for detectors of type (a) should be $A', \frac{1}{2}S'_i, (\frac{1}{2}S'_i + S'_o), A, \frac{1}{2}S_i, (\frac{1}{2}S_i + S_o)$. Using these amplitudes and substituting the values of N_a, N_b, N_c and N_d , the counts corresponding to the absorbed events are given by

$$\begin{aligned}
 N''' &= N_a''' + N_b''' + N_c''' + N_d''' \\
 &= 19N[A' + \alpha_{spi}], \tag{21}
 \end{aligned}$$

where

$$\begin{aligned}
 \alpha_{spi} &= \frac{14}{19}AS'_i + \frac{67}{114}AS'_iS_i + \frac{9}{19}AS'_iS_i^2 \\
 &= AS'_i[0.74 + 0.59S_i + 0.47S_i^2]. \tag{22}
 \end{aligned}$$

2.3 Peak-to-total and peak-to-background ratios

For addback mode, the PT of a composite detector with K module is

$$PT = \frac{KN(A' + \alpha)}{KN} = A' + \alpha. \tag{23}$$

If events escaping the composite detector get subtracted by a fraction κ (namely, suppression factor), then there is a reduction in background counts. Now, the total counts are given by

$$\begin{aligned}
 T^S &= KN - \kappa[KN - KN(A' + \alpha)] \\
 &= KN[(1 - \kappa) + \kappa(A' + \alpha)]. \tag{24}
 \end{aligned}$$

The PT and PB ratios for the suppressed detector are given by

$$PT^S = \frac{A' + \alpha}{(1 - \kappa) + \kappa(A' + \alpha)} \tag{25}$$

$$PB^S = \frac{A' + \alpha}{(1 - \kappa)[1 - (A' + \alpha)]}. \tag{26}$$

For the single detector mode, the PT and PB ratios for the suppressed detector are given by the above two equations with the condition $\alpha = 0$.

3. A procedure for extracting quantities from experimental data on cluster detector

Wilhelm *et al* have performed measurements of the fold distribution of the cluster detector for γ -rays of energies up to 10 MeV [3]. At 10 MeV, the triple-fold events contribute $\approx 17\%$ to FEP events and the contributions from four and higher fold events are negligible. In this paper, for the sake of completeness, the calculations have been performed up to four detector interactions. However, when extracting quantities from the experimental data of Wilhelm *et al* [3], we shall consider up to three-fold events due to the absence of four-fold data in the literature.

For a γ -ray of energy E_γ , let us first define the ratio of the single-detector hit events to the total full energy peak events by R_1 , the ratio of the two-detector hit events to total full energy peak events by R_2 and the ratio of three-detector hit events to total full energy peak events by R_3 . Approximate values of the detector hit ratios, the relative efficiency in addback mode ($\epsilon_{\text{rel}}^{\text{adbk}}$) and the addback factor (f) [3] are shown for three γ -ray energies in table 2. The extracted value of relative efficiency in single crystal mode ($\epsilon_{\text{rel}}^{\text{sc}}$) given by $\epsilon_{\text{rel}}^{\text{sc}} = (\epsilon_{\text{rel}}^{\text{adbk}}/f)$ is also tabulated.

If we consider eqs (12) and (13), we observe that the number of single, double and triple crystal hit events are $7N A'$, $4N S'_i A$ and $\frac{5}{2}N S'_i S_i A$, respectively. However, this theoretical observation needs consideration for multiple hit events when we are dealing with the experimental data. Experimentally, double hit events between two detectors include three and higher detector hit events between the same two detectors. For simplicity, if we include three detector hit events between the same two detectors, then the number of experimental double hit events are

$$R_2^{\text{expt}} = 3 \left(\frac{1}{3} N_1 S'_{io} A \right) + \frac{1}{3} N_1 S'_{io} \left[\frac{2}{3} S_{io} + \frac{1}{6} S_{ic} \right] + 6 \left(\frac{1}{6} N_2 S'_{ic} A \right) + 6 \left(\frac{1}{6} N_2 S'_{ic} \right) \left(\frac{1}{3} S_{io} A \right), \quad (27)$$

$$= 2N S'_i A \left(2 + \frac{1}{3} S_i \right). \quad (28)$$

Table 2. Approximate values of the detector hit ratios, the relative efficiency in addback mode ($\epsilon_{\text{rel}}^{\text{adbk}}$) and the addback factor (f) for three γ -ray energies of a cluster detector [3]. From relative efficiency in addback mode and addback factor, the value of relative efficiency in single-crystal mode ($\epsilon_{\text{rel}}^{\text{sc}}$) is extracted and is also shown.

| E_γ (MeV) | 1.3 | 3.8 | 8.0 |
|---------------------------------------|------|------|------|
| R_1 | 0.66 | 0.56 | 0.42 |
| R_2 | 0.30 | 0.38 | 0.43 |
| R_3 | 0.04 | 0.08 | 0.15 |
| $\epsilon_{\text{rel}}^{\text{adbk}}$ | 0.5 | 0.3 | 0.1 |
| f | 1.5 | 1.82 | 2.45 |
| $\epsilon_{\text{rel}}^{\text{sc}}$ | 0.33 | 0.16 | 0.04 |

Now, the number of experimental triple hit events are

$$\begin{aligned} R_3^{\text{expt}} &= \frac{5}{2} N S'_i S_i A - \frac{2}{3} N S'_i S_i A \\ &= \frac{11}{6} N S'_i S_i A \end{aligned} \quad (29)$$

If R_{21} is the ratio of the experimental double to single crystal hit events and R_{32} is the ratio of the experimental triple to experimental double crystal hit events, then

$$R_{21} = \frac{2}{7} \left(2 + \frac{1}{3} S_i \right) \frac{S'_i A}{A'} \quad (30)$$

and

$$R_{32} = \frac{11}{12} \frac{S_i}{2 + \frac{1}{3} S_i}. \quad (31)$$

Rearranging, we have

$$S_i = \frac{24 R_{32}}{11 - 4 R_{32}}. \quad (32)$$

Using this relation in eq. (32), we get

$$R_{21} = \frac{2}{7} \left(2 + \frac{8 R_{32}}{11 - 4 R_{32}} \right) \frac{S'_i A}{A'}. \quad (33)$$

4. Predictions

Using the experimental data of cluster detector hit pattern for 1.3 MeV γ -ray (table 2) as input and considering eq. (32), we get $S_i = 0.31$. Now from eq. (33), we have $A S'_i = 0.76 A'$. The experimental value of PT ratio in addback mode at 1332 keV is found to be ≈ 0.38 [2]. Using eqs (13), (23), and the above information, we get $A' = 0.25$. Now A' is proportional to the relative efficiency in single-crystal mode ($\epsilon^{\text{sd}}(E_\gamma)$), i.e., $A'(E_\gamma) \propto \epsilon^{\text{sd}}(E_\gamma)$. Now, $(A'(E_1)/\epsilon^{\text{sd}}(E_1)) = (A'(E_2)/\epsilon^{\text{sd}}(E_2))$. If $E_1 = 1.3$ MeV and $E_2 = 3.8$ MeV, then from table 2, we get $A'(3.8 \text{ MeV}) = \epsilon^{\text{sd}}(3.8 \text{ MeV}) \times [A'(1.3 \text{ MeV})/\epsilon^{\text{sd}}(1.3 \text{ MeV})] = 0.16 \times (0.25/0.33) = 0.12$. Thereafter, using the values of R_{32} and R_{21} from table 2, we extract the values of α . This process can be repeated for the 8 MeV γ -ray of table 1.

Considering eqs (13), (22), (26) and (27) we observe that the values of the three quantities – S_i , $A S'_i$ and A' are essential for determining the PT and PB ratios, as shown in table 3. So, even if values of some of the probability amplitudes remain unknown, we can still extract the values of the PT and PB ratios. Hence, we can extract FEP related information for energies where direct measurement of PT ratio is impossible due to the absence of a radioactive source having single monoenergetic γ -ray of that energy. This is an important feature of the present formalism.

The PT and PB ratios have been calculated as a function of γ -ray energy and the results are shown for cluster detector and SPI spectrometer in figure 2. Both ratios show a decreasing trend with higher γ -ray energy. The trend is similar for different modes of operation

Table 3. Approximate values of various quantities (see text) including PT ratios.

| E_γ (MeV) | 1.3 | 3.8 | 8.0 |
|---|------|------|------|
| A' | 0.25 | 0.12 | 0.03 |
| α_{cluster} | 0.13 | 0.10 | 0.04 |
| α_{SPI} | 0.17 | 0.14 | 0.06 |
| $P_{\text{adbk}}/T_{\text{adbk}}$ (cluster) | 0.38 | 0.22 | 0.07 |
| $P_{\text{adbk}}/T_{\text{adbk}}$ (SPI) | 0.42 | 0.26 | 0.09 |

and suppression cases. The improvement due to adback mode over single detector mode and suppression (here, we have considered $\kappa = 0.5$) is clearly observed.

The variation of $P_{\text{adbk}}/T_{\text{adbk}}^S$ for the cluster detector and the SPI spectrometer as a function of κ for 1.3, 3.8, and 8.0 MeV γ -rays are shown in figure 3. At 1.3 and 3.8 MeV, the PT

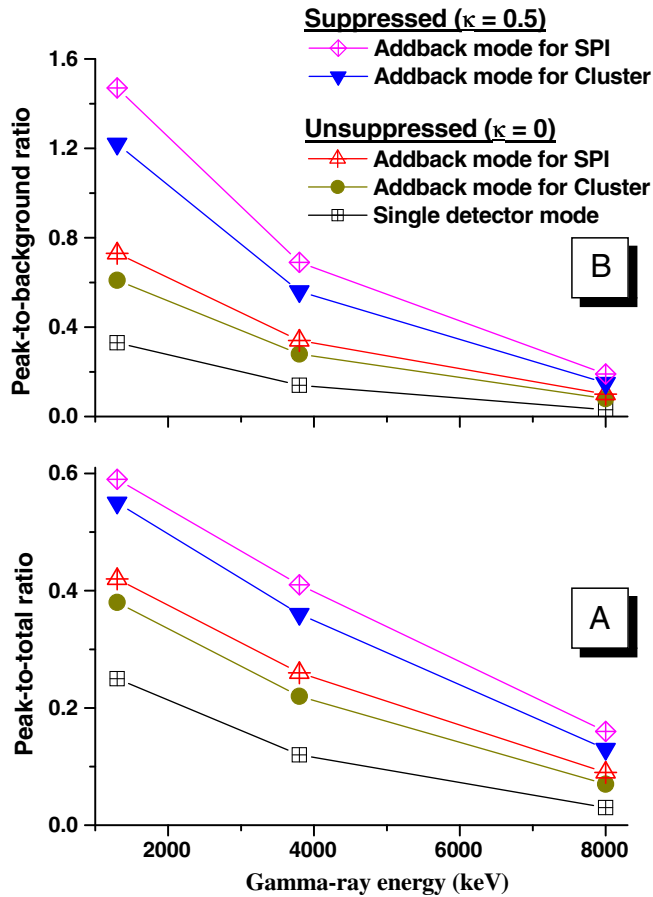


Figure 2. PT and PB ratios are plotted as a function of γ -ray energy in (A) and (B), respectively. Results are shown for various modes of operation and suppression cases for the cluster detector and SPI spectrometer.

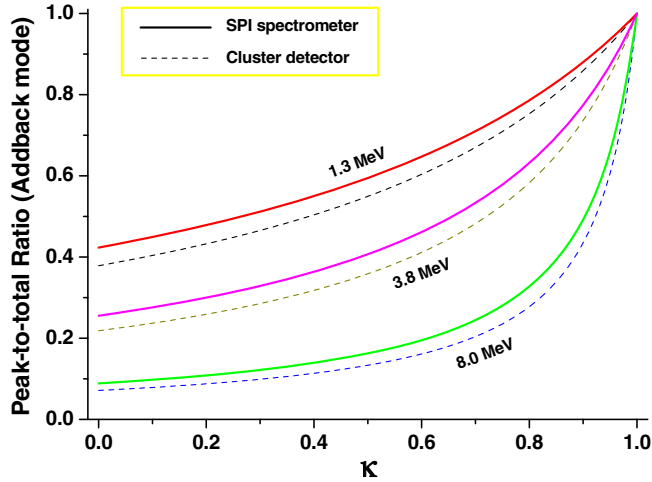


Figure 3. For observing the effect of suppression, PT ratios have been plotted as a function of κ in addback mode for three γ energies.

ratio in single crystal and addback modes increases smoothly as κ increases. For 8 MeV γ -ray, PT is quite small, up to $\kappa = 0.8$. However, due to the definition of PT ratio (see eq. (25) where PT becomes 1 when $\kappa = 1$), there is a very sharp increase after $\kappa = 0.8$.

5. Summary and conclusion

A probability model based on absorption and scattering of γ -rays, has been presented for understanding the operation of cluster and SPI detectors. In the present formalism, the operation of these sophisticated detectors could be described in terms of six probability amplitudes. Considering up to four detector interaction events, we have obtained expressions for peak-to-total and peak-to-background ratios for different suppression cases. Results indicate improved performance of the SPI spectrometer compared to the cluster detector in addback mode. It is noteworthy that for the 8 MeV energy γ -ray, there is no direct measurement of peak-to-total ratio due to the absence of a radioactive source having single monoenergetic γ -ray at that energy. This shows the importance of the present formalism in providing guidance for experimental studies with high-energy γ -rays.

References

- [1] D Attie *et al*, *Astron. Astrophys.* **411**, L71 (2003)
- [2] J Eberth *et al*, *Prog. Part. Nucl. Phys.* **38**, 29 (1997)
- [3] M Wilhelm *et al*, *Nucl. Instrum. Methods. A* **381**, 462 (1996)
- [4] R Kshetri, *Appl. Radiat. Isotopes* **75**, 30 (2013)
- [5] R Kshetri, *J. Instrum.* **7**, P04008 (2012)
- [6] R Kshetri, *J. Instrum.* **7**, P07006 (2012)
- [7] R Kshetri, *J. Instrum.* **7**, P12007 (2012)
- [8] R Kshetri, *J. Instrum.* **7**, P07008 (2012)
- [9] R Kshetri, *J. Instrum.* **7**, P08015 (2012)